




Tectonics of the Neuchâtel Jura Mountains: insights from mapping and forward modelling

Valentin Rime¹  · Anna Sommaruga¹ · Marc Schori¹ · Jon Mosar¹

Received: 16 October 2018 / Accepted: 25 September 2019 / Published online: 11 October 2019
© The Author(s) 2019

Abstract

This study focuses on a geological section in the Jura Mountains across the villages of Travers, La Brévine in Switzerland, and Morteau in France. Field mapping was conducted to complement and densify existing data. A kinematically and geometrically consistent forward model has been developed to understand and interpret the observed surface structures. The proposed solution features a low-angle thrust fault with a multiple ramp-flat or staircase trajectory on which several hinterland-verging thrusts nucleate. The main décollement level is located in the Triassic evaporites of the Keuper and Muschelkalk Groups. Our model implies secondary detachments in the Opalinus Clay and the Cretaceous layers leading to repetitions in the Mesozoic cover rocks over large distances. This in turn explains the high topographic position of exposed sediments. The proposed solution is an alternative to models showing overthickening of Triassic evaporites associated with a single detachment level. Along the investigated profile, the Jura Mountains accommodate a shortening of 8.5 km. The kinematic forward model suggests an oscillating sequence of thrusting, rather than a simple, in sequence, forward propagation succession of thrusts.

Keywords Fold-and-thrust belt · Thin-skinned tectonics · Balanced cross-section · Secondary detachment · Ramp-flat geometry · Staircase trajectory

1 Introduction

The Jura Mountains are the north-northwestern foreland fold-and-thrust belt related to the Alpine orogeny (Buxtorf 1907; Burkhard and Sommaruga 1998). The latter is associated to the closure of the Alpine Tethys induced by the subduction of the European plate towards the south and the subsequent collision with the Adriatic plate (Escher and Beaumont 1997; Stampfli et al. 1998; Stampfli and Borel 2002). The Jura Mountains are surrounded by three Cenozoic sedimentary basins (see Fig. 1). The Molasse

Basin in the south initiated as a flexural basin north of the Alpine orogeny in early Oligocene and evolved into a detached wedge-top basin (Homewood et al. 1986; Willett and Schlunegger 2010; Gruber 2017; Sommaruga et al. 2017). The Bresse Graben to the west, and the Rhine Graben to the north are part of the European Cenozoic Rift System, which formed in Eocene and Oligocene times (Ziegler 1992; Dèzes et al. 2004).

The uplift and imbrication of the External Crystalline Massifs, which started in the late Oligocene (Burkhard 1990; Burkhard and Sommaruga 1998; Leloup et al. 2005; Pfiffner 2014), initiated the detachment and deformation of the northern Alpine foreland comprising the Molasse Basin and the Jura fold-and-thrust belt (FTB). The basal décollement level is located in the Triassic evaporites of the Keuper and Muschelkalk Groups (Buxtorf 1907; Burkhard 1990; Jordan 1992; Philippe et al. 1996; Sommaruga 1997; Mosar 1999; Sommaruga et al. 2017; see Fig. 2). The relatively low overburden due to the northward pinching out of Molasse sediments and the presence of a rheologically weak décollement level promoted the deformation by thin-skinned folding and thrusting in the Jura

Editorial Handling: A. Pfiffner.

Electronic supplementary material The online version of this article (<https://doi.org/10.1007/s00015-019-00349-y>) contains supplementary material, which is available to authorized users.

✉ Valentin Rime
valentin.rime@unifr.ch

¹ Department of Geosciences, University of Fribourg, Chemin du Musée 6, 1700 Fribourg, Switzerland

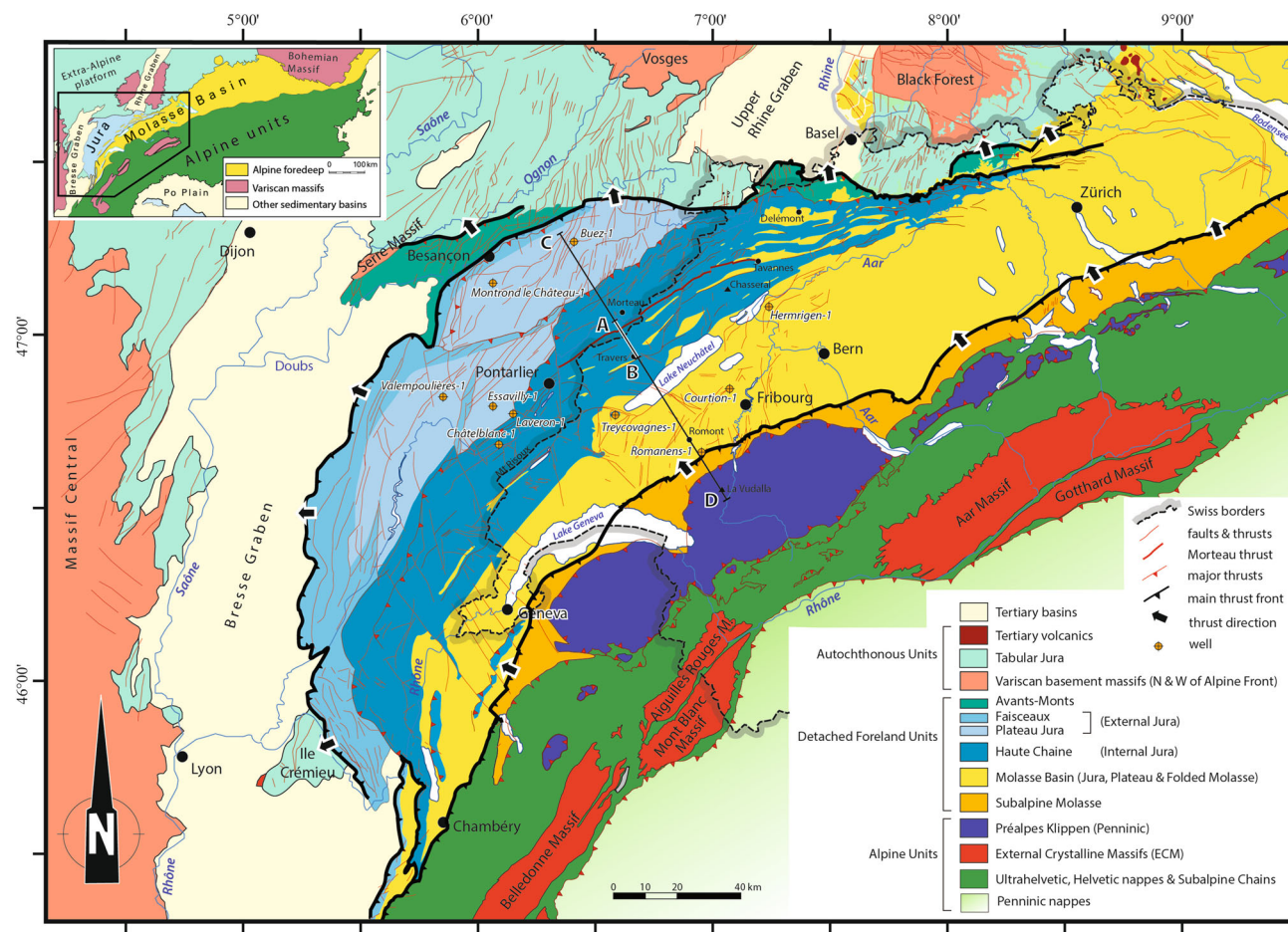


Fig. 1 Overview map of the Jura fold-and-thrust belt and the Molasse Basin. Trace A–B: cross-section Fig. 5, 8, trace C–D: cross-section Fig. 6 and trace A–D: cross-section Fig. 10. Modified after Sommaruga et al. (2017)

FTB and the Molasse Basin (Philippe et al. 1996; Sommaruga 1999; Sommaruga et al. 2017). This deformation is explained by the “Fernschub” theory (after Buxtorf 1907) linking emplacement of the External Crystalline Massifs to the initiation of the main décollement. Several authors argued for a recent transition to thick-skinned deformation along with a mild inversion of Permo-carboniferous grabens (Mosar 1999; Ustaszewski and Schmid 2007; Madritsch et al. 2008; Pfiffner 2014).

The area of investigation is located NW of Lake Neuchâtel in the most deformed part of the Jura, the Internal Jura or Haute Chaîne Jura, characterised by large-scale thrusts and related folds (Figs. 1 and 2). It extends from the village of Travers in the canton of Neuchâtel to the vicinity of the city of Morteau in the Doubs department in France, crossing the Vallée de La Brévine (Figs. 3 and 4). The regional elevations are about 1300 m along the anticlinal summits and 730–1000 m in the synclinal valleys. These elevations imply significant tectonic thickening. First investigations in the region date back to De Montmollin in 1839, whilst numerous structural cross-sections were

published during the first half of the XXth century (Schardt and Dubois 1903; Schardt 1907; Rickenbach 1925; Thiébaud 1937; Frei 1946). After British Petroleum conducted a seismic survey in the area in 1988 and shared the data with the academic community, several cross-sections showing the deep structures were published (Sommaruga 1997, 2011; Groupe de travail PGN 2008; Pasquier et al. 2013). The quality of seismic lines acquired on Swiss territory is, however, rather low and interpretations of deep structures therefore suffer from significant uncertainties. While all authors agree on a thin-skinned tectonic style, different solutions explaining the tectonic thickening of the sedimentary cover were proposed. We based our investigation on the geological maps 1:50'000 of Morteau by Fallot et al. (1968) and the 1:25'000 Swiss geological map of Travers (Pasquier and Burkhard 2013) complemented by fieldwork to solidify structural data along the modelled section.

The aim of this study was to produce a kinematically plausible model of the Neuchâtel Jura Mountains and its neighbouring French part using forward modelling

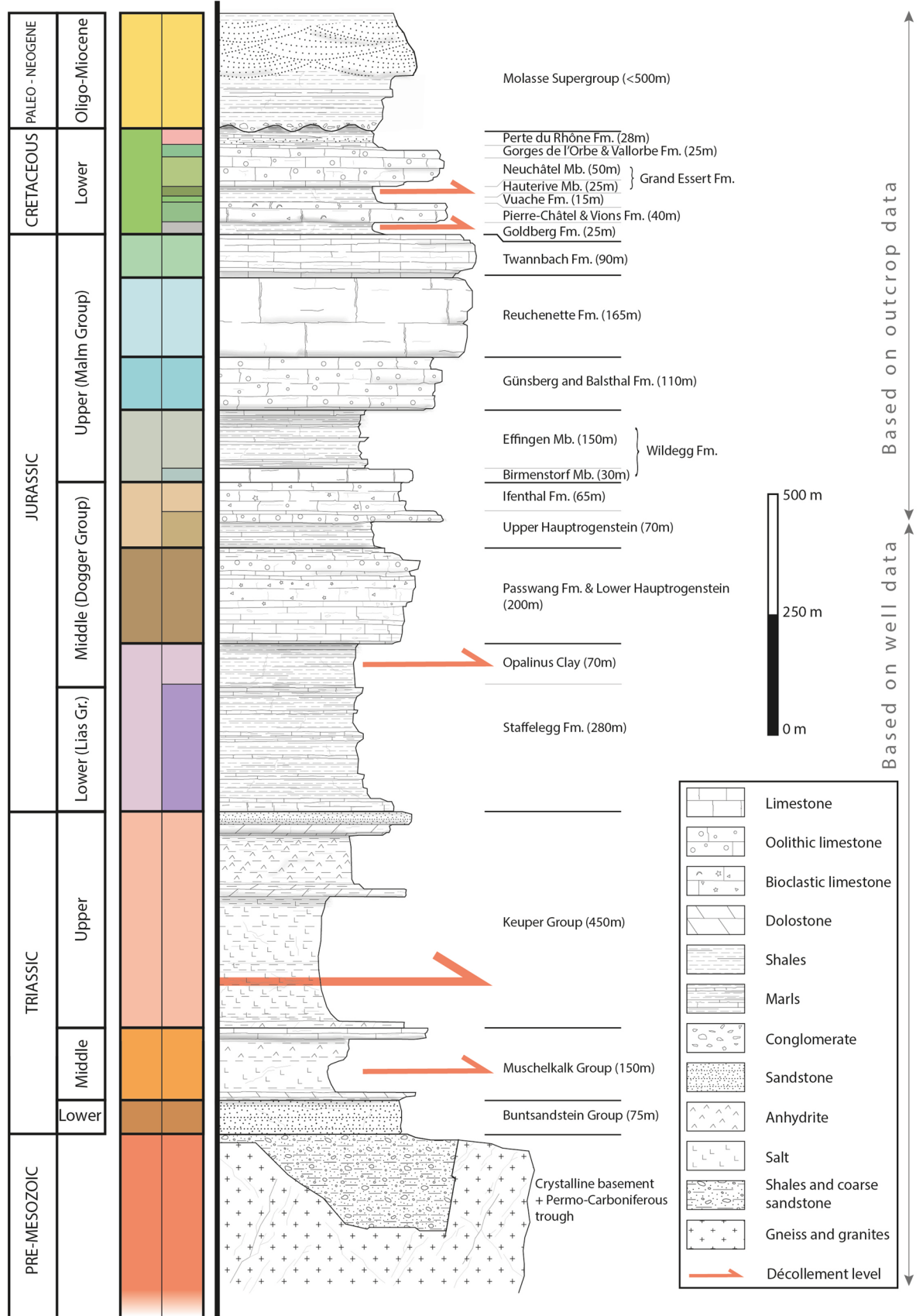
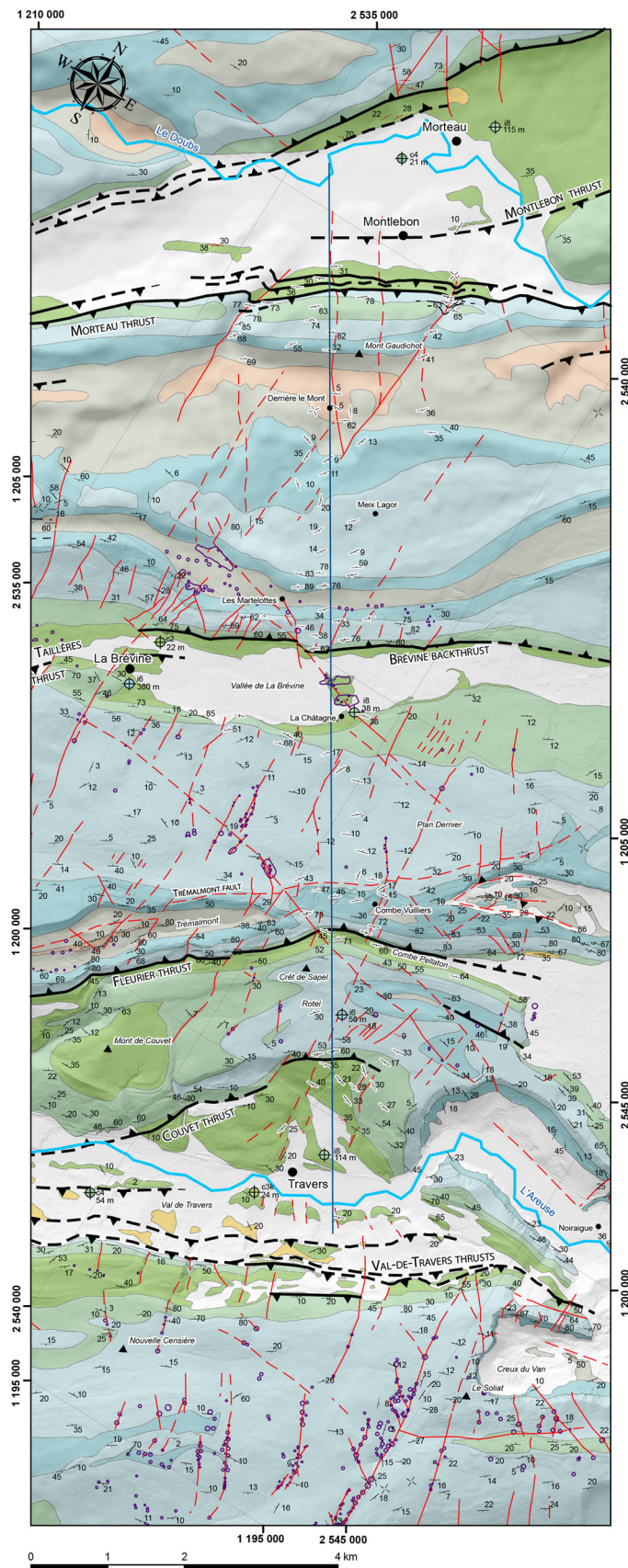


Fig. 2 Stratigraphic log of the study area based on field observations, Pasquier et al. (2013) and data of the wells presented on Fig. 1



GEOLOGICAL MAP

TRAVERS - LA BRÉVINE - MORTEAU
SWITZERLAND - FRANCE

INTERNAL JURA - JURA FOLD-AND-THRUST BELT

Symbols

- Bedding direction (with dip angle)
- Horizontal bedding
- Vertical bedding
- Overturned bedding (with dip angle)
- Bedding from Pasquier and Burkhard (2013) and Fallot et al. (1968) (with dip angle)
- Bedding from Sommaruga (1997) (with dip angle)
- Doline
- Well (with unit color and code and depth of the roof)

- Fault
- Fault (supposed or buried)
- Thrust
- Thrust (supposed or buried)
- Section trace

Geological Units

- Quaternary
- Molasse
- Cretaceous
- Twannbach Fm.
- Reuchenette Fm.
- Günsberg and Balsthal Fm.
- Wildeggen Fm.
- Upper Hauptrogenstein & Ifenthal Fm.

Sources

Geology modified after:

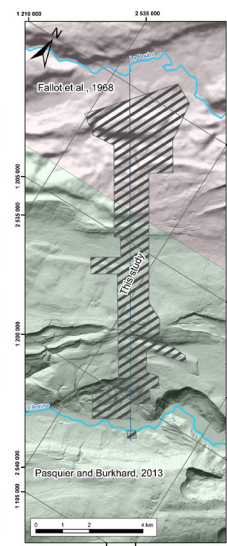
Pasquier, F. and Burkhard, M. (2013). 1163 Travers. Atlas Géologique de la Suisse 1:25'000, Federal Office of Topography swisstopo, 162.

Fallot, P., Perrodon, A., Umbach-Bascone, P., Fortems, G., Tixier, M., Cassedanne, J., Sainton, C., Ziegler, M., Nicklès, M., Aubert, D., Bourquin, P., and Glangeaud, L. (1968). Feuille XXXV-24, Morteau. Carte géologique détaillée de la France, 1/50'000.

DEM:

SwissAlti3D by Swisstopo

EU-DEM (Produced using Copernicus data and information funded by the European Union)



◀**Fig. 3** Simplified geological map of the study area with focus on the pre-Quaternary rocks. Based on Fallot et al. (1968) and Pasquier and Burkhard (2013) with observations of this study. Note that the section trends NNW-SSE. Coordinate system: CH1903 LV95. Available in higher resolution and with more details (1:25'000) in Online Resource 1

techniques (Mugnier et al. 1990; Mount et al. 1990; Schori et al. 2015).

2 Stratigraphy

The underground of the study area is made of pre-Mesozoic basement (s.l.), including Permocarboniferous half-grabens, covered by Mesozoic and Cenozoic sediment. In the study area, only the upper part of the stratigraphic column is known from field observations (younger than Lower Jurassic, see Fig. 2). The description of Pasquier et al. (2013), compiled for the geological map Travers (Pasquier and Burkhard 2013), was used for the outcropping units. The deeper stratigraphic column (from the Lower Hauptrogenstein downwards) was compiled based on data from several deep wells drilled in the Jura Mountains and in the Molasse Basin (Valempoulières-1, Essavilly-1, Laveron-1, Châtelblanc-1, Montrond le Château-1, Treycovagnes-1, Buez-1, Courtion-1 and Hermrigen-1, see Fig. 1). The closest well, Treycovagnes-1, is located more than 15 km to the SW. A thin layer of Quaternary deposits, which was not considered during modelling in this work, forms the uppermost part of the stratigraphic column. The Paleogene-Neogene siliciclastic Molasse sediments unconformably (foredeep unconformity) overlie Lower Cretaceous marls and limestones. The underlying Upper Jurassic unit includes Upper Malm Group, mostly made of massive limestones forming most of the outcrops in the study area and Lower Malm Group marls and argillaceous sediments. They in turn cover limestones and marly limestones of the Dogger Group. The lowermost Dogger Group unit, the Opalinus Clay, is mainly composed of mudstones and marls and forms a mechanically weak layer (Nussbaum et al. 2011; Schori et al. 2015). The Triassic rocks of the Keuper and Muschelkalk Groups consist largely of evaporites (anhydrite, gypsum and halite), marls, limestones and dolomites. Note that the stratigraphy of the Triassic sediments was recently revised by Jordan (2016). The evaporites host the main décollement level. According to Jordan (1992), Pfiffner (2014), Gruber (2017) and Sommaruga et al. (2017), most of the deformation is concentrated in the evaporites of the Keuper Group in the western and central Jura and in the Muschelkalk Group in the eastern Jura. The study area is situated in the central Jura, near to the transition of these two domains. Finally, the continental sandstones of the Buntsandstein Group overlie

the top of the basement, thus resting on the Variscan age peneplain surface. Together with the Paleozoic and older crystalline rocks (gneisses and granites) and Permo-Carboniferous continental sediments locally deposited in tectonic half-grabens, they are regarded as mechanical basement and form the foot-wall to the main décollement.

3 Methodology

In order to investigate and construct a geological section we combined new field data with existing information and seismic data into a new profile that was subsequently reconstructed by forward modelling.

3.1 Surface geology and mapping

The published geological maps (Fallot et al. 1968; Pasquier and Burkhard 2013) were combined in a local geological map focusing on tectonic structures and pre-Quaternary sediments (Fig. 3), and in a regional tectonic map (Fig. 4) with our field measurement, as well as structural data from Sommaruga (1997), an analysis of high resolution topographic data (SwissAlti3D by swisstopo and SRTM by NASA/NGA), shallow well data (Pasquier et al. 2013) and the results of a geophysical study (radiomagnetotelluric by Pasquier, 2008; Pasquier and Turberg, 2009). A near-surface cross-section (Fig. 5) was also elaborated based on the combined datasets. More than 75% of the field measurements were collected within 700 m of the cross-section.

3.2 Seismic data analysis

One seismic line (SW88-07) acquired in 1988 by British Petroleum (BP) crosses the study area and has been interpreted by Sommaruga (1997, 1999, 2011). The poor quality of this line can be explained by “the steep topography and the karstification of the Jurassic limestones” (Sommaruga 1997). Hereafter, the interpretation by Sommaruga (1997, 2011) was used to assign the stratigraphic units to the different seismic facies, but a new seismic velocity model was applied to convert the horizons from time to depth (Table 1) using MoveTM package. From studies in the northern Alpine foreland, Sommaruga et al. (2012, 2016) estimate the depth uncertainty up to ± 300 m (see also Gruber 2017 for discussion).

3.3 Forward modelling

The general workflow of forward modelling was inspired by Mount et al. (1990). Modelling was done in the MoveTM software by Midland Valley (now Petroleum Experts) using the 2D Move-on-Fault tool of the 2D Kinematic

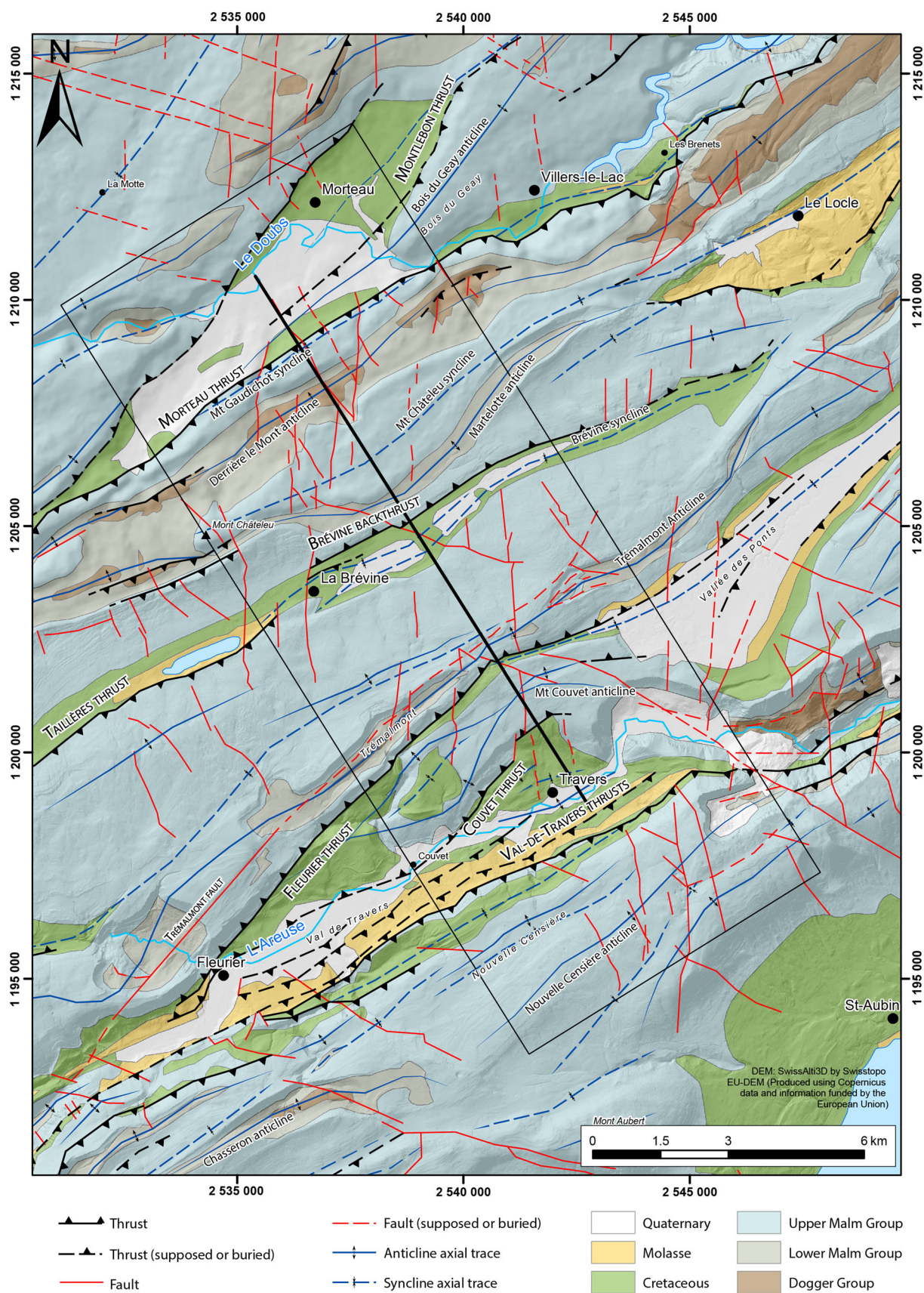


Fig. 4 Regional tectonic map of the study area. The black rectangle indicates the location of the geological map (Fig. 3) and the thick black line represents the position of the cross-section (A–B on Fig. 1). Based on Fallot et al. (1968), Rollier and Favre (2010), Pasquier and Burkhard (2013), Eichenberger et al. (2019) and the present study. Coordinate system: CH1903 LV95

Modelling module. This tool produces deformation based on the geometry of a fault drawn by the user. Three different methods were used:

(a) Trishear (Erslev 1991) postulates a distributed shear in a triangular shear zone in front of a propagating fault and is area balanced. It implies thickness changes in the shear zone, which are known from folds in the Jura Mountains (e.g. Schardt 1901, Nussbaum et al. 2011). Trishear uses Fault Parallel Flow (Egan et al. 1997; Kane et al. 1997) to model deformation behind the triangular shear zone. Fault Parallel Flow might produce minor thickness changes over folds.

(b) The Fault-bend Fold (Suppe 1983) method assumes gliding of the hanging wall on the fault without layer thickness change but does not allow to model the steep or overturned forelimbs observed in the study area. Fault-propagation folds were therefore modelled with the Trishear algorithm.

A trial and error modelling approach proved to be efficient to reconstruct the fault-related folds of the study area.

4 Results

The main results concern the shallow structural section, the position of the top of the basement and the modelled and final cross-section (Figs. 5, 6, 7, 8, 9).

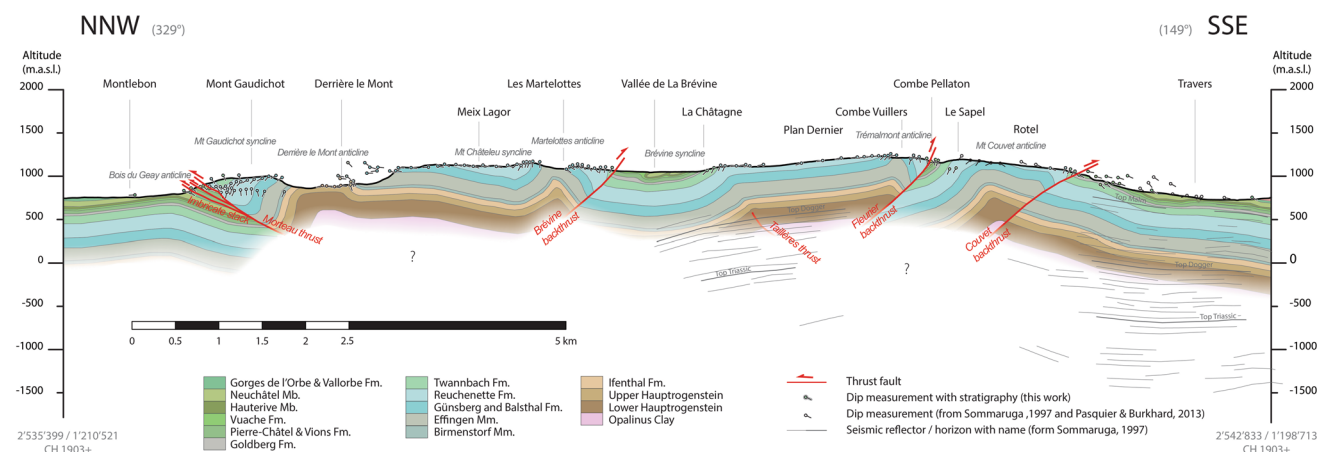


Fig. 5 Initial shallow interpretation of the structures based on field measurements, existing geological maps (Fallot et al. 1968; Pasquier and Burkhard 2013), structural data from Sommaruga (1997), DEM analysis, shallow well data (Pasquier et al. 2013) and geophysical studies (Pasquier 2008; Pasquier and Turberg 2009). Seismic reflector horizons from Sommaruga (1997) were converted to depth with a new

Table 1 Seismic velocities used in this work, based on comparison of data from Sommaruga 1997; Sommaruga et al. 2012; Pasquier et al. 2013; Gruber 2017

Unit	Velocity (m/s)
Cenozoic	2500
Cretaceous	3600
Malm group	4800
Dogger and lias groups	4200
Triassic	4500
Basement	5000

4.1 Shallow structures

The shallow structures and lithologies (see maps and section in Figs. 3, 4 and 5) show a succession of high-amplitude folds related to major thrusts and backthrusts. The relatively high structural and topographic elevation of the Mesozoic and Cenozoic series between the Morteau thrust and the Couvet backthrust is a major feature of this area. Our structural interpretation of the Swiss territory is very similar to the understanding of Pasquier and Burkhard (2013). In the French part of the investigated area the densification of data from fieldwork helped refine the structural interpretation on the map of Fallot et al. (1968).

The southern part of the study area is characterised by two hinterland-verging thrusts: the Couvet and Fleurier backthrusts (Figs. 3, 4, 5). Because of the constant NNW-dipping layers, the Combe Pellaton structure was interpreted as a monocline rather than a syncline as suggested by Pasquier and Burkhard (2013). The subvertical Trémalmont fault (Fig. 3), introduced by Pasquier and

velocity model. Discrepancies between the section and the seismic line result from the lateral offset of the seismic line and the cross-section trace (the line was shot 1.5 km east of the section in the Vallée de La Brévine and 1 km west of the section near Travers). This near-surface cross-section was the base on which the forward model was built. The position of the cross section is shown in Fig. 4

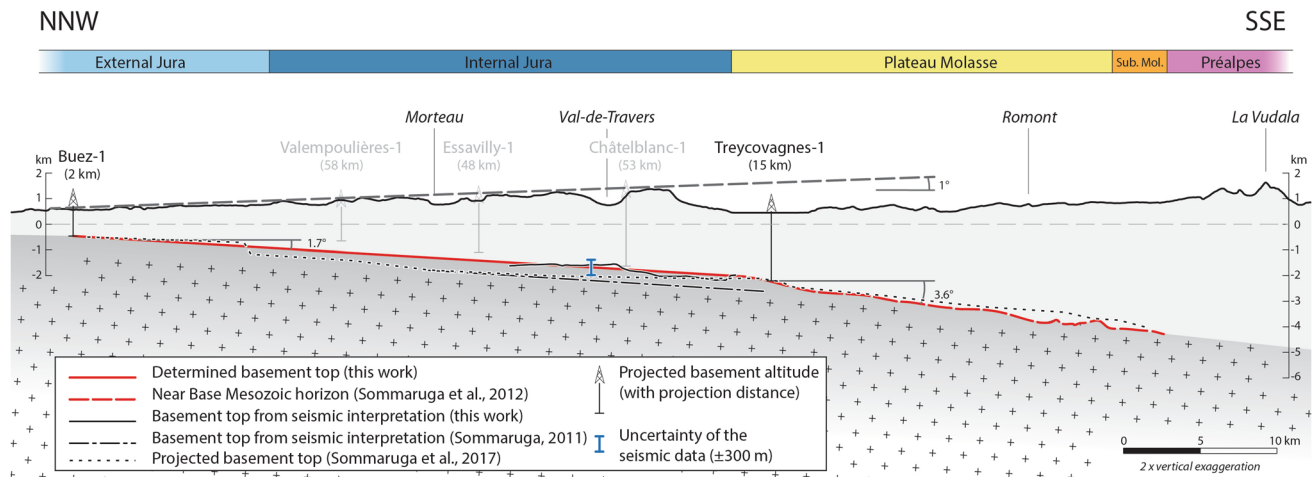


Fig. 6 Proposed geometry of the top basement based on a comparison with well data and interpretations by Sommaruga (2011) and Sommaruga et al. (2012, 2017). See Fig. 1 for a map view. The wells are projected into the section with an azimuth of 60°, parallel to the fold axes. The greyed-out wells lie more than 45 km to the west of the Pontarlier fault system. The top basement horizon from Sommaruga et al. (2017) represents the situation interpreted 14 km west of the study area. The blue error bars represent the depth

uncertainty of ± 300 m discussed in the text. We can observe that the “Near Base Mesozoic” horizon from Sommaruga et al. (2012) in the Molasse Basin, the wells Treycovagnes-1 and Buez-1 and the interpretation proposed herein are consistent. The dip of the top basement interface increases towards the SE from 1.7° in the Internal and External Jura to approx. 3.6° under the Plateau Molasse. The topographic slope of the Jura Mountains is 1° toward the north

Burkhard (2013), could neither be observed in the field, nor did the DTM show any conclusive evidence about its presence. A “supposed fault” was therefore indicated in our map and it was not considered in our cross-section. The steeply dipping layers observed in La Châtagne, on the southern side of the La Brévine valley (Figs. 3, 5), are probably related to a fold associated with the Taillères thrust mapped by Pasquier and Burkhard (2013) further west. In the Vallée de La Brévine, the Cretaceous layers form second order, small and tight folds (Fig. 5; Pasquier 2008). These folds are probably restricted to the well-layered Cretaceous series where the high rheological heterogeneity of marls and limestones and the regular spacing of bedding promote layer-parallel slip and “out of the syncline thrusting” (McClay 1992). Similar folds are described in the same series farther east, near the city of Fleurier (Droxler and Schaer 1979). North of the Brévine backthrust, the Martelottes anticline, the Mt Châtelet syncline and the Derrière le Mont anticline (Figs. 3, 4, 5) are not disturbed by any visible significant fault. The structure of the Mt Gaudichot (Fig. 5) differs significantly from the interpretation of Fallot et al. (1968), where this structure is mapped and interpreted to entirely form the northern limb of the Derrière le Mont anticline. Fieldwork and refined analysis show that the entire mountain forms a tight syncline whose northern flank is cut by several foreland-verging thrusts leading to stacking of the Cretaceous layers (Figs. 3, 5). This thrust system was called the Morteau thrust and forms an imbricate stack. Fallot et al. (1968) do not map this thrust and instead interpret this area as the

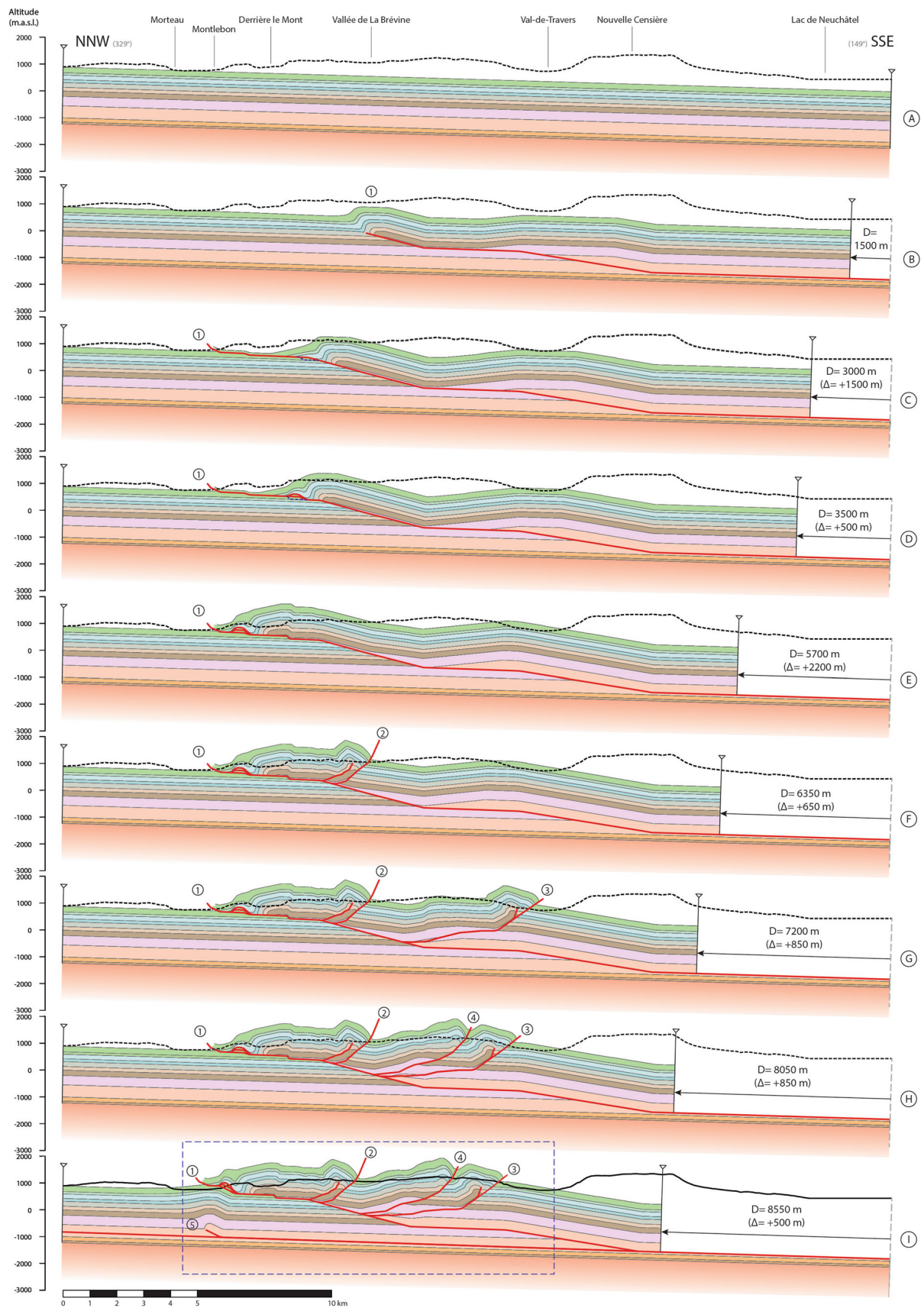
southern limb of a broad syncline forming the Morteau valley. This is neither consistent with bedding, nor with the superposition of the different units (see Online Ressource 1). North of the city of Morteau, the steep, foreland-verging beds are overturned and most likely linked with a hinterland-verging thrust system (Figs. 3, 4).

The study area is dissected by three sets of strike-slip faults. The first set, associated with sinistral movement, shows a N–S orientation (Fig. 3). The second set, associated with dextral movement, shows a WNW–ESE orientation and hence, represents the conjugate of the first set. The third set shows NNW–SSE orientations, perpendicular to the general trend of the fold axes, and is interpreted here to represent extensional fractures.

4.2 Basement

In order to model a detached and deformed cover series it was essential to determine the position, dip and topography of the pre-Mesozoic rocks. Our knowledge of the basement topography (Wildi and Huggenberger 1993; Philippe et al. 1996; Madritsch et al. 2008; Sommaruga 1997) strongly depends on the quality and resolution of geophysical data.

Fig. 7 Kinematic forward model of the study area. D: total shortening; Δ : incremental shortening. Numbers represent the chronology of thrusts: 1: Morteau thrust, 2: Brévine and Martelottes backthrusts, 3: Couvet backthrust, 4: Fleurier backthrust, 5: Montlebon thrust. The blue rectangle in section I shows the outline of the sections presented in Fig. 8 and the limits of the study area. The stratigraphy is shown in Fig. 2



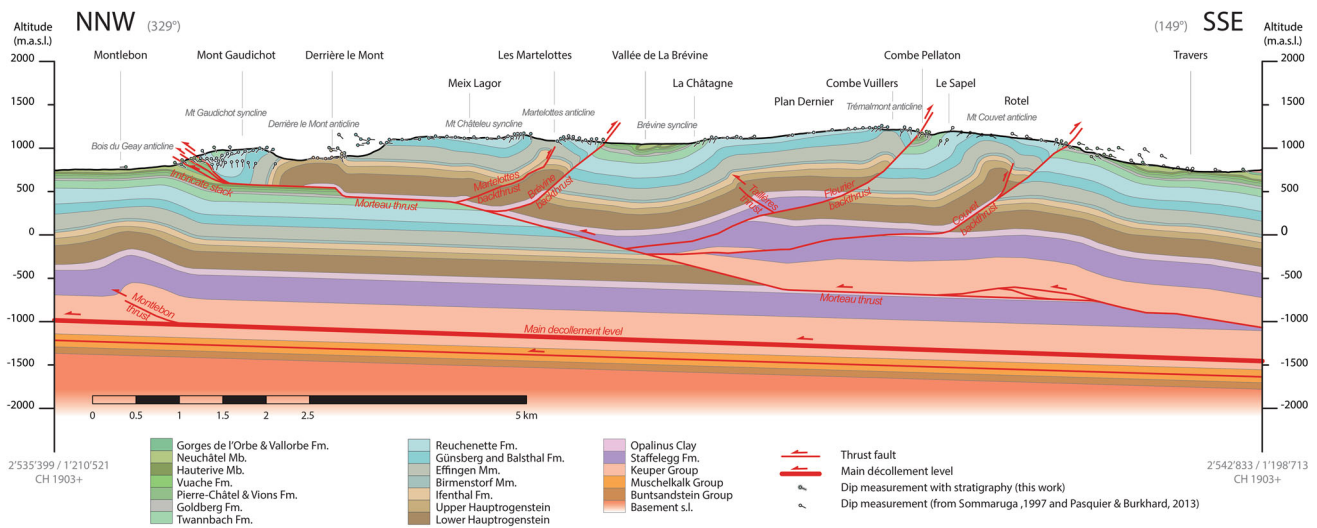
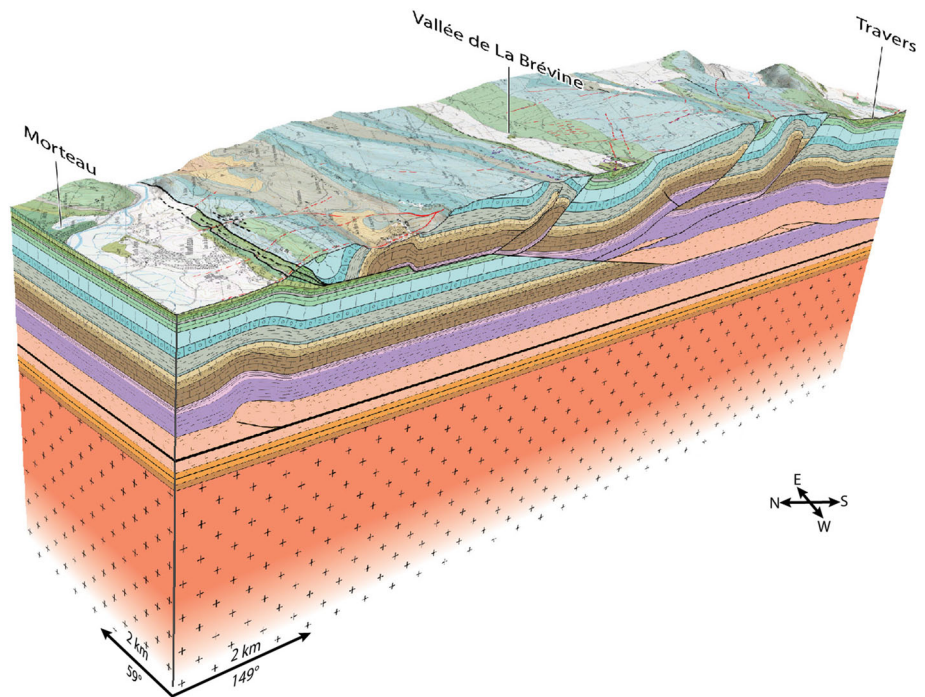


Fig. 8 Final cross-section with dip data. This interpretation is a compromise between the forward model (see Fig. 7, step I) and surface data (Fig. 5). The location of the cross-section is represented

in Figs. 1, 3 and 4. Two block-diagrams of this cross-section are shown in Fig. 9 and Online Resource 2

Fig. 9 Block-diagram of the cross-section (Fig. 8) combined with the geological map (Online Resource 1). See the corresponding figures for the legends



Earth magnetic anomalies (Meyer et al. 2017), gravimetric data (Olivier et al. 2002; BRGM 2009) and seismic reflection data (Sommaruga 1997) were reviewed. No dataset showed distinct signals, which could be interpreted as a clear signature of the top basement or the basement topography. Thus, in absence of reliable information, a basement without topography was considered for this study.

The depth to the top of the mechanical basement was determined based on well data, particularly the

Treycovagnes-1 and Buez-1 wells, seismic data reprocessed with a new velocity model and existing basement models such as in Sommaruga et al. (2012) for the Molasse Basin.

These different data yield depths varying by no more than 300–400 m depths (Fig. 6). The position of the basement was chosen to comply with these data, with emphasize on the ones with small projection distances.

4.3 Forward modelling

The aim of the forward model was to produce a geometrically and kinematically plausible cross-section of the study area, based on the surface cross-section that reproduces, as much as possible, all known data (Fig. 5). Forward modelling was applied to explore and test different assumptions on the fault sequence and geometry. It can be demonstrated that a specific chronology of activation of thrusts yields a given final geometry. Therefore, the preferred final model contains kinematic information on the fold and thrust development. The final model presented (Fig. 7) matches the observations to a high degree, but does not exclude the possibility of alternative solutions.

Based on regional studies and interpretations (e.g. Sommaruga 1997; Pasquier et al. 2013) we consider that the general deformation style is thin-skinned, with thrust-related folding. The décollement is most likely concentrated in the halite layers of the Lower Keuper Group, as shown by well data (Jordan 1992) and thickness variations (Gruber 2017; Sommaruga et al. 2017), although deformation is expected to be partitioned between the Keuper and the Muschelkalk Groups. For modelling purposes, the Keuper Group layers were considered to host a single discrete basal décollement level. Based on field observations and well data, it appears realistic to consider a constant stratigraphic thickness of the Mesozoic sequence over the study area for the model.

An important issue to solve was the origin of the considerable tectonic thickening above the basal décollement between the Val-de-Travers and the Mt Gaudichot (Fig. 5). The elevation of the Cretaceous series in the Val-de-Travers (~ 730 m a.s.l.) and in the Morteau valley (~ 750 m a.s.l.) corresponds to a more or less normal stratigraphic stack of the sedimentary cover over the basement. The considerably higher elevations in-between, even in the synclines such as the Combe Pellaton and the Vallée de La Brévine (~ 1000 m a.s.l.), are due to structural uplifts (Fig. 5).

The final model (Fig. 7) solves this issue by applying a multiple ramp-flat or staircase geometry (after McClay 1992) to the main thrust (Morteau thrust) rooting in the Keuper Group and featuring secondary detachments in the Opalinus Clay and the marly Cretaceous layers, connected by low-angle ramps. This geometry involves large displacements, explains the uplift of the sedimentary cover and leads locally to repetitions of the Mesozoic sequence over large distances. Another outcome of applying this geometry is the possibility to develop shallower detachment levels on which smaller structures can form. It was impossible to model the relatively small scale Mt Couvet

and Tremalmont anticlines with thrusts rooting in the Keuper Group.

In our forward model (Fig. 7), the Morteau thrust first forms a fault-propagation fold (step B, fault 1) and later evolves into a fault-bend fold (C–E), forming an imbricate stack. Subsequently, branching off the main thrust, a series of backthrusts develop, forming first the Brévine, and then the Martelottes backthrust (F, 2), the Couvet backthrust (G, 3) and finally the Fleurier backthrust (H, 4). The Martelottes thrust and the splay of the Couvet backthrust were modelled to explain the steep backlimbs of the related folds. A steep backlimb can also be explained by pop-up structures, but due to software limitations, it was not possible to model such a geometry. An equivalent of the Couvet splay was mapped further to the east (Pasquier and Burkhard 2013; Fig. 3). Finally, the deformation propagates along the basal décollement level where it forms a small blind thrust below the village of Montlebon (Fig. 7; step I, thrust fault 5). This latter thrust is more developed to the NE, forming the Bois du Geay anticline (Fig. 4; Philippe et al. 1996).

4.4 Final cross-section

The final cross-section (Figs. 8, 9) is a compromise between the forward model (Fig. 7) and the surface cross-section (Fig. 5). Though the forward model represents a geometrically and kinematically plausible reconstruction of the deep structures, fitting surface data to a high degree, the near-surface cross-section is more precise at shallow depth. Therefore the final cross-section (Figs. 8, 9) has been elaborated by integrating relevant near surface structures into the modelled section to obtain a more accurate and admissible section. Thus, a small duplex structure was added to the meridional part of the forward model beneath the Rotel summit (Mt Couvet anticline) to better represent the low-amplitude fold in the footwall of the Couvet backthrust (Fig. 8). Furthermore, a foreland-verging thrust (the Taillères thrust) rooting in the Fleurier backthrust was added below Plan Dernier to account for the steeper bedding observed in La Châtaine (Fig. 8). This thrust was impossible to model due to software limitations.

5 Discussion

5.1 Tectonic structure

The proposed structure shows a thin-skinned thrust-related deformation rooting in the basal Triassic units décollement level (Keuper Group). Modelling shows that no basement topography is needed to explain the structural elevation of the outcropping rocks, especially in the central portion of

the section (Vallée de La Brévine). Instead, the elevated position of layers is explained by the large-scale Morteau thrust, which accommodates 5.7 km of shortening according to our kinematic model. The presence of such a major thrust is only conceivable if the lateral extent of the thrust is also substantial (Kim and Sanderson 2005). Although this thrust is neither represented on the Swiss Tectonic Map 1:500'000 (Federal Office for Water and Geology 2005), nor on the Morteau map (Fallot et al. 1968), data from various sources (Muhlethaler 1930; Bourquin et al. 1946, 1968; BRGM 1969; Pascal 1975; Burger and Schaer 1996; Sommaruga 1997; Groupe de travail PGN 2008; Rollier and Favre 2010; Aufranc and Burkhalter 2017) allow us to conclude that it most likely extends from the N–S Pontarlier strike-slip fault in the west, to the village of Tavannes in the east (Fig. 1), over more than 60 km. This is consistent with the significant displacement predicted by our model. Furthermore, imbricate stacks are often found in the forelimb of large-scale ramp-flat thrusts (e.g. Boyer 1992).

The Morteau thrust features a secondary detachment in the Opalinus Clay and two others in the Cretaceous marly layers, in the Goldberg Formation and in the Marnes bleues d'Hauterive. The Opalinus Clay detachment is a crucial feature of our model. The Opalinus Clay consists of a shaly and a sandy facies, both featuring high clay content (Bossart et al. 2017) and thus forming a mechanically weak layer capable of hosting major deformation. In the Chasseral area, Aufranc et al. (2017) propose a very similar model with the “Chasseral nappe” featuring a low angle flat-ramp-flat where the Opalinus Clay and the Cretaceous layers form flats. Schori et al. (2015) (and references therein) also model the Chasseral anticline of the Haute Chaîne with a major secondary detachment in the Opalinus Clay layers. Furthermore, Hossack (1979) recognized this phenomenon in the eastern Jura Mountains where “Most thrusts propagate first from the basal décollement in the Middle Triassic evaporites to the Opalinus shales”. In the same region, Malz et al. (2016) recognized that this layer is possibly hosting secondary detachments. In the Risoux area of the Central Jura, Laubscher (1965); Philippe et al. (1996) and Endignoux and Mugnier (1990) also propose cross-sections where the Opalinus Clay or the Lias Group act as secondary detachment. Finally, numerical models in foreland fold-and-thrust belts using two weak detachment levels (Stockmal et al. 2007) demonstrate a tendency for longer thrust segments to form in the lower detachment. We consider that these results further support the model proposed here for the Jura FTB. The numerical models further imply that the décollement levels, as is the case in the Jura FTB, must be very weak. This also holds true for the Jura FTB, even if there is a difference in mechanical strengths between the Triassic evaporites and the shaly

Cretaceous and Opalinus Clay detachment (Jordan 1992; Sommaruga et al. 2017).

The staircase geometry resulting from these secondary detachments leads to fault-bend folds and yields large displacements, which cause a stacking and repetition of the Mesozoic sequence over large distances (Zoetemeijer and Sassi 1992; Medwedeff and Suppe 1997). This explains the structural thickening of the sedimentary cover in this part of the Jura Mountains. It is an alternate solution to models where the high elevation of the rocks is explained salt tectonics, implying important thickening of the Triassic evaporites. While mechanically plausible, this thickening would require more important shortening in the Triassic units than in the overlying units. This is not plausible since both the Triassic and the post-Triassic sediments accommodate the same shortening, unless all deformation in the décollement level is accommodated by flow. Interpretation of seismic data from the Molasse Basin (Sommaruga 1999) suggest deformation by duplexing.

The study area comprises three major backthrusts, which are common in foreland fold-and-thrust belts (Bonini 2007), and well recognized in the Jura Mountains (e.g. Sommaruga 1997; Pasquier et al. 2013; Rigassi 2011; Aufranc et al. 2017). The backthrusts in the study area develop above the Morteau thrust, possibly for wedge equilibrium reasons (Davis et al. 1983) and because the movement over ramps leads to the development of backthrusts (e.g. Erickson et al. 2001; Rosas et al. 2017). The presence of salt and anhydrite in the Jura FTB strongly reduces basal friction (Davis and Engelder 1985) and the basal coupling, thus allowing the fold-and-thrust belt to develop a narrow cross-sectional taper of about 2.7° (Fig. 6). Therefore, the mechanically favourably oriented thrusts have similar dips and backthrusting is promoted (Davis and Engelder 1985), in agreement with our observations in the Jura FTB. Analogue modelling experiments (Costa and Vendeville 2002; Schreurs and Colletta 2002; Couzens-Schultz et al. 2003; Smit et al. 2003; Bonini 2007; Bonnet et al. 2007, 2008; Buitier 2012) have confirmed this mechanical model, although the brittle-ductile decoupling is not the sole factor explaining the vergence of the thrusts (Smit et al. 2003; Bonini 2007). The model proposed here bears similarities with models showing intermediate brittle-ductile coupling (Smit et al. 2003; Buitier 2012) where the foreland-vergent thrusts dominate, but where major backthrusts have a strong influence on the general structure. The steeper backthrusts are also consistent with an intermediate brittle-ductile coupling according to both, theoretical and analogue models.

The Morteau thrust appears to control the deformation of the whole study area, over a distance of more than 10 km, similarly to the Val-de-Travers thrust, which controls the structure between the study area and the Lac de

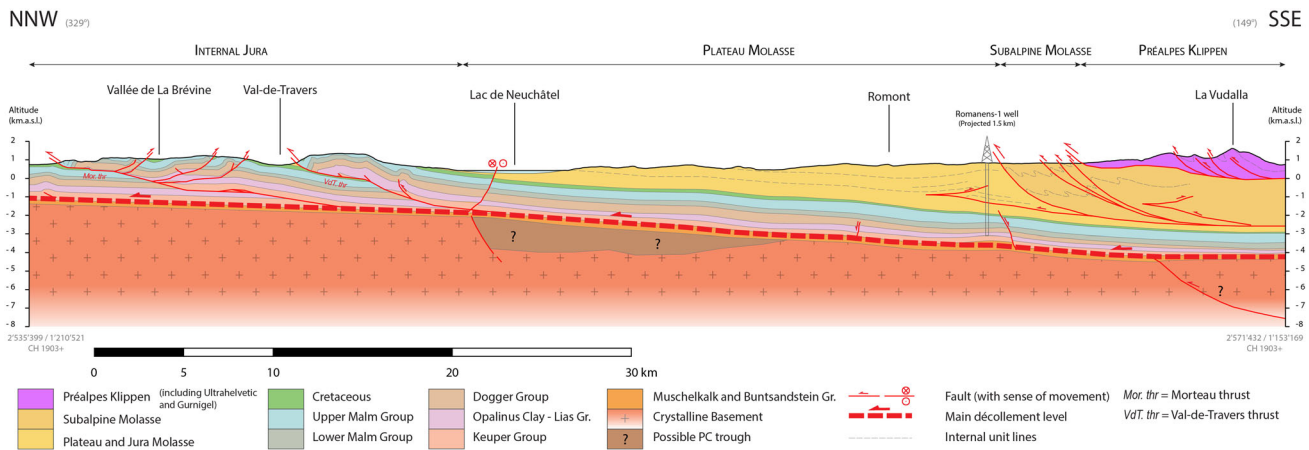


Fig. 10 Regional cross-section through the study area in the NNW, the Molasse Basin and the Préalpes in the SSE. The NNW portion up to the Val-de-Travers is based on the present work. The section between the Val-de-Travers and Lake Neuchâtel is based on seismic data, modified after Sommaruga (2011) and Gruber (2017). The Plateau Molasse is based on the 3D MoveTM model by Gruber (2017). The Subalpine Molasse and the Préalpes is compiled from Pugin

(1951); Federal Office for Water and Geology (2005); Matzenauer (2012); Mosar et al. (2014) and Gruber (2017). The location of the cross-section is given in Fig. 1. A block-diagram of this cross-section is available in Online Resource 3. Further lithospheric scale cross-sections are presented in Federal Office for Water and Geology (2005) and Pfiffner (2014)

Neuchâtel (Fig. 10). We propose that the Internal Jura is segmented into nappes. These are controlled by major large-scale low-angle forward-verging thrusts accommodating much of the shortening and leading to tectonic thickening in the Internal Jura Mountains. A similar development of nappes was proposed in the Risoux area by Aubert (1971), Bitterli (1972) and Wildi and Huggenberger (1993) and in the Chasseral area by Aufranc et al. (2017).

5.2 Kinematic model

The sequential kinematic model (Fig. 7) correlates with a total shortening of 8.55 km for the study area, which corresponds to 33% of relative shortening. This result is in agreement with the value of 8.8 km obtained by Philippe et al. (1996) for an equivalent cross-section 5 km to the NE of the section presented here. A total shortening of 21 km for the whole belt as proposed by Philippe et al. (1996) and of 26 km by Burkhard and Sommaruga (1998) can thus be considered realistic.

The geometry of folds and thrusts reflects the sequential development of the structures. Conversely, the search of a succession of thrusts and folds that leads to the observed geometries reflects the temporal development. Following a series of exploratory reconstructions, we modelled the structures in the area of investigation from north to south (back-breaking sequence) so that a structure modelled in the south is not reworked with each step further north. Two exceptions to this are the Couvet and Fleurier backthrusts, modelled in a forward-breaking sequence because it was impossible to obtain a correct structure at Plan Dernier without the structure previously formed by the Couvet

backthrust and the late formation of the Montlebon thrust (Fig. 8). Since all backthrusts root in the Morteau thrust (1), the Morteau thrust must have formed first. As seen before, the timing of the Couvet backthrust relative to the Fleurier backthrust is constrained by geometrical reasons. The exact timing of the Montlebon thrust is unknown but the fact that it influences the geometry of the Morteau thrust, the Mt Gaudichot syncline and the Cretaceous unit imbricate stack, suggests that it was formed after the Morteau thrust.

Thus, the proposed reconstruction shows an overall oscillating sequence of thrusting. According to Smit et al. (2003), this is related to an intermediate brittle-ductile coupling, in accordance with the geometry of tectonic structures and the cross-sectional taper (see above).

6 Conclusion

Field mapping, in combination with published maps and data from literature such as well logs and seismic profiles, helped to gain a better understanding of the structures in the central Jura FTB along a Travers-La Brévine-Morteau transect in the Swiss and French Jura Mountains. Forward modelling techniques exploring and testing different assumptions on the fault sequence and geometry were applied to construct a coherent kinematic and structural model of the subsurface, allowing us to produce a balanced cross-section. The model highlights several key points of the tectonics of the area:

(a) Based on our modelling, we suggest that a secondary detachment in the middle Jurassic Opalinus Clay plays a

key role along with a main basal décollement over the mechanical basement in the Triassic evaporite layers (Keuper Group). This secondary detachment and the large displacement accommodated by the ramp-flat style Mor-teau thrust allows to explain the high topographic elevation of the layers in the central part of the section. These upper detachments are responsible for the important tectonic thickening of the sedimentary cover observed in the internal Jura Mountains. No basement topography is required to explain the elevated topographic position of the layers and surface. Our modelling does, however, not explicitly exclude such a possibility.

(b) Major thrusts such as the Mor-teau thrust to the north of the study area or the Val-de-Travers thrust to the south delimit nappe-like tectonic units that subdivide the Haute Chaîne Jura.

(c) Along the studied profile, the Jura Mountains accommodate a shortening of 8.5 km, corresponding to a relative shortening of some 33%.

(d) The comparison of the structural style and the thrust propagation sequence in our model are supported by the tapered wedge theory and analogue experiments. The weak Triassic evaporites and the small taper lead to an intermediate brittle-ductile coupling yielding dominant foreland verging thrusts with major backthrusts and an oscillating sequence of thrusting.

Acknowledgements We are thankful to Jeremiah Mauvilly and Léa Perrochet for their help during fieldwork and to Marius Gruber, Bruno Lauper and Robin Fentimen for their help and support. We also thank H. Madritsch, O. A. Pfiffner and an anonymous reviewer for their constructive and helpful comments, which contributed significantly to the improvement of the manuscript. We gratefully acknowledge Petroleum Experts for providing the software MOVE which was used for the cross-section construction and forward modelling.

Open Access This article is distributed under the terms of the Creative Commons Attribution 4.0 International License (<http://creativecommons.org/licenses/by/4.0/>), which permits unrestricted use, distribution, and reproduction in any medium, provided you give appropriate credit to the original author(s) and the source, provide a link to the Creative Commons license, and indicate if changes were made.

References

- Aubert, D. (1971). Le Risoux, un charriage jurassien de grandes dimensions. *Eclogae Geologicae Helveticae*, 64, 151–156.
- Aufranc, J. and Burkhalter, R. (2017). Feuille 1125 Chasseral. Atlas géol. Suisse 1:25 000, Carte 155, Federal Office of Topography, swisstopo.
- Aufranc, J., Jordan, P., Piquerez, A., Hofmann, B., Anders, B. and Burkhalter, R. (2017). Feuille 1125 Chasseral. Atlas géol. Suisse 1:25 000, Notice expl. 155, Federal Office of Topography, swisstopo.
- Bitterli, P. (1972) Erdölgeologische Forschungen im Jura, Bulletin der Vereinigung Schweiz. Petroleum-Geologen und-Ingenieure, 39, 13–28.
- Bonini, M. (2007). Deformation patterns and structural vergence in brittle-ductile thrust wedges: an additional analogue modelling perspective. *Journal of Structural Geology*, 29, 141–158.
- Bonnet, C., Malavielle, J. and Mosar, J. (2007). Interactions between tectonics, erosion, and sedimentation during the recent evolution of the Alpine orogen: Analogue modelling insights. *Tectonics*, 26, TC6016.
- Bonnet, C., Mosar, J., & Malavielle, J. (2008). Surface processes versus kinematics of thrust belts: impact on rates of erosion, sedimentation, and exhumation- Insights from analogue models. *Bulletin de la Société Géologique de France*, 179(3), 297–314.
- Bossart, P., Bernier, F., Birkholzer, J., Bruggeman, C., Connolly, P., Dewonck, S., et al. (2017). Mont Terri rock laboratory, 20 years of research: introduction, site characteristics and overview of experiments. *Swiss Journal of Geosciences*, 110, 3–22.
- Bourquin, P., Buxtorf, R., Frei, E., Luthi, C., Muhlethaler, C., Ryniker, K., and Suter, H. (1968). Feuille 1144 Val de Ruz. Atlas Géologique de la Suisse 1:25 000, Carte 51, Federal Office of Topography swisstopo.
- Bourquin, P., Suter, H., and Fallot, P. (1946). Feuille 1124 Biaufond-Les Bois-La Ferrière- St Imier. Atlas Géologique de la Suisse 1:25 000, Carte 15, Federal Office of Topography swisstopo.
- Boyer, S. E. (1992). Geometric evidence for synchronous thrusting in the southern Alberta and northwest Montana thrust belts. In K. R. McClay (Ed.), *Thrust Tectonics* (pp. 377–390). Dordrecht: Springer.
- BRGM. (1969). Pontarlier, (557). *Carte géologique détaillée de la France*, 1(50), 000.
- BRGM (2009). Anomalie de Bouguer. Réseau et carte gravimétrique de la France 2009, RCGF09.
- Buiter, S. J. H. (2012). A review of brittle compressional wedge models. *Tectonophysics*, 530, 1–17.
- Burger, A. and Schaer, J.-P. (1996). La vallée du Locle—oasis jurassienne. Avec une carte géologique 1:50 000. Cahiers de l'Institut neuchâtelois.
- Burkhard, M. (1990). Aspects of the large-scale Miocene deformation in the most external part of the Swiss Alps (sub-Alpine molasse to Jura fold belt). *Eclogae Geologicae Helveticae*, 83, 559–583.
- Burkhard, M., & Sommaruga, A. (1998). Evolution of the western Swiss Molasse basin: structural relations with the Alps and the Jura belt. *Geological Society, London, Special Publications*, 134, 279–298.
- Buxtorf, A. (1907). Zur Tektonik des Kettenjura. Bericht der Versammlung des Oberrheinischen Geologischen Vereins, 40.
- Costa, E., & Vendeville, B. C. (2002). Experimental insights on the geometry and kinematics of fold-and-thrust belts above weak, viscous evaporitic décollement. *Journal of Structural Geology*, 24, 1729–1739.
- Couzens-Schultz, B. A., Vendeville, B. C., & Wiltshko, D. V. (2003). Duplex style and triangle zone formation: insights from physical modeling. *Journal of Structural Geology*, 25, 1623–1644.
- Davis, D. M., & Engelder, T. (1985). The role of salt in fold-and-thrust belts. *Tectonophysics*, 119, 67–88.
- Davis, D., Suppe, J., & Dahlen, F. A. (1983). Mechanics of Fold-and-Thrust Belts and Accretionary Wedges. *Journal of Geophysical Research*, 88, 1153–1172.
- De Montmollin, A. (1839). Note explicative pour la Carte géologique de la principauté de Neuchâtel. Mémoires de la Société des Sciences Naturelles de Neuchâtel, 2.
- Dèzes, P., Schmid, S. M., & Ziegler, P. A. (2004). Evolution of the European cenozoic rift system: interaction of the Alpine and Pyrenean orogens with their foreland lithosphere. *Tectonophysics*, 389, 1–33.

- Droxler, A., & Schaer, J.-P. (1979). Déformation cataclastique plastique lors du plissement, sous faible couverture, de strates calcaires. *Eclogae Geologicae Helveticae*, 72, 551–570.
- Egan, S.S., Buddin, T.S., Kane, S., Williams, G.D. (1997). Three dimensional modelling and visualisation in structural geology: New techniques for the restoration and balancing of volumes. In: Proceedings of the 1996 Geoscience Information Group Conference on Geological Visualisation (pp. 67–82). Electronic Geology.
- Eichenberger, U., Pictet, A., & Gogniat, S. (2019). Feuille 1143 L Locle et 1123 Le Russey.—Atlas géol. Suisse 1:25 000, Federal Office of Topography, swisstopo (**in preparation**).
- Endignoux, L., & Mugnier, J.-L. (1990). The use of a forward kinematic model in the construction of balanced cross sections. *Tectonics*, 9, 1249–1262.
- Erickson, S. G., Strayer, L. M., & Suppe, J. (2001). Initiation and reactivation of faults during movement over a thrust-fault ramp: numerical mechanical models. *Journal of Structural Geology*, 23, 11–23.
- Erslev, E. A. (1991). Trishear fault-propagation folding. *Geology*, 19, 617–620.
- Escher, A., & Beaumont, C. (1997). Formation, burial and exhumation of basement nappes at crustal scale: a geometric model based on the Western Swiss-Italian Alps. *Journal of Structural Geology*, 19, 955–974.
- Fallot, P., Perrodon, A., Umbach-Bascone, P., Fortems, G., Tixier, M., Cassedanne, J., et al. (1968). Feuille XXXV-24, Morteau. *Carte géologique détaillée de la France*, 1(50), 000.
- Federal Office for Water and Geology (2005). Carte tectonique de la Suisse 1:500 000.
- Frei, E. (1946). 3 coupes géologique a travers la feuille No 279, Noiraigue, de l'atlas topographique Siegfried. Unpublished, Available at the Institute for Geology of the University of Neuchatel.
- Groupe de travail PGN (2008). Evaluation du potentiel géothermique du canton de Neuchatel. CREGE 11-08/02, Neuchâtel.
- Gruber, M. (2017). Structural Investigations of the Western Swiss Molasse Basin - From 2D Seismic Interpretation to a 3D Geological Model. *GeoFocus*, 41, 190 pp.
- Homewood, P., Allen, P. A., & Williams, G. D. (1986). Dynamics of the Molasse Basin of western Switzerland. *Special Publications International Association Sedimentologists*, 8, 199–217.
- Hossack, J. R. (1979). The use of balanced cross-sections in the calculation of orogenic contraction: a review. *Journal of the Geological Society*, 136, 705–711.
- Jordan, P. (1992). Evidence for large-scale decoupling in the Triassic evaporites of Northern Switzerland: an overview. *Eclogae Geologicae Helveticae*, 85, 677–693.
- Jordan, P. (2016). Reorganisation of the Triassic stratigraphic nomenclature of northern Switzerland: overview and the new Dinkelberg, Kaiseraugst and Zeglingen formations. *Swiss Journal of Geosciences*, 109, 241–255.
- Kane, S.J., Williams, G.D., Buddin, T.S., Egan, S.S., Hodgetts, D. (1997). Flexural-slip based restoration in 3D, a new approach. 1997 AAPG Annual Convention Official Program, A58.
- Kim, Y.-S., & Sanderson, D. J. (2005). The relationship between displacement and length of faults: a review. *Earth-Science Reviews*, 68, 317–334.
- Laubscher, H.-P. (1965). Ein kinematisches Modell der Juraufaltung. *Eclogae Geologicae Helveticae*, 58, 232–318.
- Leloup, P. H., Arnaud, N., Sobel, E. R., & Lacassin, R. (2005). Alpine thermal and structural evolution of the highest external crystalline massif: the Mont Blanc. *Tectonics*, 24, 1–26.
- Madritsch, H., Schmid, S. M., and Fabbri, O. (2008). Interactions between thin- and thick-skinned tectonics at the northwestern front of the Jura fold-and-thrust belt (eastern France). *Tectonics*, 27, TC5005.
- Malz, A., Madritsch, H., Meier, B., and Kley, J. (2016). An unusual triangle zone in the external northern Alpine foreland (Switzerland): Structural inheritance, kinematics and implications for the development of the adjacent Jura fold-and-thrust belt. *Tectonophysics*, 670, 127–143.
- Matzenauer, E. (2012). Tectonics of the Préalpes Klippen and the Subalpine Molasse (Canton Fribourg, Switzerland). *GeoFocus*, 31, 210.
- McClay, K. R. (1992). Glossary of thrust tectonic terms. In *Thrust Tectonics*, 419–434.
- Medwedeff, D. A., & Suppe, J. (1997). Multibend fault-bend folding. *Journal of Structural Geology*, 19, 279–292.
- Meyer, B., Saltus, R., & Chulliat, A. (2017). *EMAG2: Earth Magnetic Anomaly Grid (2-arc-minute resolution) Version 3*. Maryland: National Centers for Environmental Information, NOAA.
- Mosar, J. (1999). Present-day and future tectonic underplating in the western Swiss Alps: reconciliation of basement/wrench-faulting and decollement folding of the Jura and Molasse basin in the Alpine foreland. *Earth and Planetary Science Letters*, 173, 143–155.
- Mosar, J., Abednego, M., Gruber, M., and Sommaruga, A. (2014). Tectonics between the Préalpes Klippen and the Swiss western Molasse Basin in the Bulle region (Fribourg). Poster Swiss Geoscience Meeting.
- Mount, V. S., Suppe, J., & Hook, S. C. (1990). A Forward Modeling Strategy for Balancing Cross Sections. *AAPG Bulletin*, 74, 521–531.
- Mugnier, J.-L., Guellec, S., Menard, G., Roure, F., Tardy, M., & Vialon, P. (1990). A crustal scale balanced cross-section through the external Alps deduced from the ECORS profile. *Mémoires de la Société géologique de France*, 156, 203–216.
- Muhlethaler, C. (1930). Feuille 1162 La Chaux - Les Verrières. Atlas Géologique de la Suisse 1:25'000, Carte 2, Federal Office of Topography, swisstopo.
- Nussbaum, C., Bossart, P., Amann, F., & Aubourg, C. (2011). Analysis of tectonic structures and excavation induced fractures in the Opalinus Clay, Mont Terri underground rock laboratory (Switzerland). *Swiss Journal of Geosciences*, 104, 187–210.
- Olivier, R., Dumont, B., Barrios, L., Klingelc, E., Logean, P., Perret, F., and Rosset, P. (2002). Atlas Gravimétrique Suisse au 1:100 000. Office fédéral de topographie, swisstopo.
- Pascal (1975). Fiche Signalétique du Tunnel de Lachenoy (identifiant BSS001KYPK). Banque du Sous-Sol (BSS), BRGM.
- Pasquier, F. (2008). Campagne géophysique RMT pour la feuille 1163 Travers de l'Atlas géol. Suisse 1:25'000. Rapp. Serv. Géol. Nat., Swisstopo, Wabern (unpublished).
- Pasquier, F. and Burkhard, M. (2013). Feuille 1163 Travers. Atlas Géologique de la Suisse 1:25 000, Carte 162, Federal Office of Topography, swisstopo.
- Pasquier, F., Burkhard, M., Mojon, P.-O., and Gogniat, S. (2013). Feuille 1163 Travers. Atlas Géologique de la Suisse 1:25 000, Atlas Géologique de la Suisse 1:25 000, Notice expl. 162, Federal Office of Topography, swisstopo.
- Pasquier, F., & Turberg, P. (2009). *Use of the Radiomagnetotelluric method in Quaternary mapping*. Bern: Abstract for CH-QUAT Meeting.
- Pfiffner, O. A. (2014). *Geology of the Alps*. Chichester: John Wiley & Son.
- Philippe, Y., Colletta, B., Deville, E., & Mascle, A. (1996). The Jura fold-and-thrust belt: a kinematic model based on map-balancing. *Mémoires du Muséum national d'histoire naturelle*, 170, 235–261.
- Pugin, L. (1951). Profils géologiques de la région du Molson entre Gruyères et Albeuve. *Eclogae Geologicae Helveticae*, 44.

- Rickenbach, E. (1925). 18 Profils équidistants a travers la région du Val-de-Travers. *Bulletin de la Société neuchâteloise des sciences naturelles*, 50.
- Rigassi, D. (2011). Feuille 1182 Ste-Croix. Atlas géol. Suisse 1:25 000, Notice epxl. 95, Federal Office of Topography, swisstopo.
- Rollier, J. and Favre, J. (2010) Carte géologique des environs du Locle et de la Chaux-de-Fonds, 1:25'000, Carte géol. spéciale 59, Federal Office of Topography, swisstopo.
- Rosas, F. M., Duarte, J. C., Almeida, P., Schellart, W. P., Riel, N., & Terrinha, P. (2017). Analogue modelling of thrust systems: passive vs. active hanging wall strain accommodation and sharp vs. smooth fault-ramp geometries. *Journal of Structural Geology*, 99, 45–69.
- Schardt, H. (1901). Les mouvements de rocher à la Clusette. *Bulletin de la Société des sciences naturelles de Neuchâtel*, 29, 108–119.
- Schardt, H. (1907). *Geologisches Profil*. Val de Travers-Saint Aubin: Deposited in the Unit of Earth Sciences, University of Fribourg.
- Schardt, H., & Dubois, A. (1903). Description géologique de la région des Gorges de l'Areuse (Jura neuchâtelois). *Eclogae Geologicae Helvetiae*, 7, 367–476.
- Schori, M., Mosar, J., & Schreurs, G. (2015). Multiple detachments during thin-skinned deformation of the Swiss Central Jura: a kinematic model across the Chasseral. *Swiss Journal of Geosciences*, 108, 327–343.
- Schreurs, G., & Colletta, B. (2002). Analogue modelling of continental transpression. *Journal of the virtual Explorer*, 7, 103–114.
- Smit, J. H. W., Brun, J. P., and Sokoutis, D. (2003). Deformation of brittle-ductile thrust wedges in experiments and nature. *Journal of Geophysical Research: Solid Earth*, 108.
- Sommaruga, A. (1997). Geology of the Central Jura and the Molasse basin: New insight into an evaporite-based foreland fold and thrust belt. *Mémoires de la Société Neuchâteloise de Sciences Naturelles*, 12, pp. 176.
- Sommaruga, A. (1999). Décollement tectonics in the Jura foreland fold-and-thrust belt. *Marine and Petroleum Geology*, 16, 111–134.
- Sommaruga, A. (2011). From the central Jura Mountains to the Molasse Basin (France and Switzerland). *Swiss Bulletin für angewandte Geologie*, 16, 63–75.
- Sommaruga, A., Eichenberger, U., & Marillier, F. (2012). *Seismic Atlas of the Molasse Basin*. Swiss Geological Survey: Federal Office of Topography swisstopo.
- Sommaruga, A., Gruber, M., and Mosar, J. (2016). Synthèse des données géologiques utiles pour la construction d'un modèle du sous-sol du Canton de Fribourg. *GeoFocus*, 39, pp. 103.
- Sommaruga, A., Mosar, J., Schori, M., and Gruber, M. (2017). The role of the Triassic evaporites underneath the North Alpine foreland. In Soto, J., Flinch, J., and Tari, G., (Ed.), *Permo-Triassic salt provinces of Europe, North Africa and the Atlantic Margins: tectonics and hydrocarbon potential*, chapter 22 (IV). Elsevier.
- Stampfli, G. M., & Borel, G. D. (2002). A plate tectonic model for the Paleozoic and Mesozoic constrained by dynamic plate boundaries and restored synthetic oceanic isochrons. *Earth and Planetary Science Letters*, 196, 17–33.
- Stampfli, G., Mosar, J., Marquer, D., Marchant, R., Baudin, T., & Borel, G. (1998). Subduction and obduction processes in the Swiss Alps. *Tectonophysics*, 296, 159–204.
- Stockmal, G. S., Beaumont, C., Nguyen, M., & Lee, B. (2007). Mechanics of thin-skinned fold-and-thrust belts: insights from numerical models. *Geological Society of America Special Papers*, 433, 63–98.
- Suppe, J. (1983). Geometry and kinematics of fault-bend folding. *American Journal of Science*, 283, 684–721.
- Thiébaud, C.-E. (1937). Etude géologique de la région de Travers, Creux du Van, St-Aubin. *Bulletin de la Société neuchâteloise des sciences naturelles*, 45, 5–76.
- Ustaszewski, K., & Schmid, S. M. (2007). Latest Pliocene to recent thick-skinned tectonics at the Upper Rhine Graben—Jura Mountains junction. *Swiss Journal of Geosciences*, 100, 293–312.
- Wildi, W., & Huggenberger, P. (1993). Reconstitution de la plateforme européenne antéorogénique de la Bresse aux Chaînes Subalpines; éléments de cinématique alpine (France et Suisse occidentale). *Eclogae Geologicae Helvetiae*, 86, 47–64.
- Willeit, S. D., & Schlunegger, F. (2010). The last phase of deposition in the Swiss Molasse Basin: from foredeep to negative-alpha basin. *Basin Research*, 22, 623–639.
- Ziegler, P. A. (1992). European Cenozoic rift system. *Tectonophysics*, 208, 91–111.
- Zoetemeijer, R., & Sassi, W. (1992). 2-D reconstruction of thrust evolution using the fault-bend fold method. In K. R. McClay (Ed.), *Thrust Tectonics* (pp. 133–140). Dordrecht: Springer.